ELSEVIER

Contents lists available at ScienceDirect

International Journal of Solids and Structures

journal homepage: www.elsevier.com/locate/ijsolstr



From octagonal connection graphs belonging to the Z-Octahedron family to new tensegrity structures



Manuel Alejandro Fernández-Ruiz ^{a,*}, Enrique Hernández-Montes ^b, Luisa María Gil-Martín ^b

- a Department of Industrial and Civil Engineering. University of Cádiz (UCA). Campus Bahía de Algeciras. Avda. Ramón Puvol, s/n. 11201 Algeciras (Cádiz). Spain
- ^b Department of Structural Mechanics, University of Granada (UGR), Campus Universitario de Fuentenueva s/n. 18072 Granada, Spain

ARTICLE INFO

Keywords: Tensegrity Z-Octahedron family Octagonal cell Analytical form-finding Force density method

ABSTRACT

A tensegrity family is a group of tensegrity structures that share a common connectivity pattern. The Octahedron, the Z-Octahedron, and the X-Octahedron families are examples of these groups found in the literature. In this work, a new graphical representation of the members of the Z-Octahedron family based on octagonal cells is presented. These new elementary cells are composed of eight nodes and two struts. In addition, a new member of the family is introduced: the Z-triple-expanded octahedron. New tensegrity structures from the Z-Octahedron family are obtained by modifying the connectivity pattern of the elements that make up the octagonal cell. Several element groupings have been considered in order to find different equilibrium configurations. The values of the force density or force:length ratio that lead to stable and super-stable tensegrity forms have been computed analytically. It has been proved that the Z-Octahedron family is a good source of new tensegrity forms.

1. Introduction

Tensegrity structures are pin-jointed, free-standing, and pre-stressed, and they are composed of compression (struts) and tension (cables) members that are self-equilibrated. The unique mechanical and mathematical properties of these structures mean that they have applications in many fields, such as robotics (Graells Rovira and Mirats Tur, 2009; Lee et al., 2020; Liu et al., 2022), biology (Fraldi et al., 2021; Suma et al., 2020), mechanical engineering (Boni and Royer-Carfagni, 2021; Kan et al., 2019), civil engineering (Bel Hadj Ali et al., 2010; Veuve et al., 2016), and aerospace engineering (Chen et al., 2020; Tibert and Pellegrino, 2002). Tensegrity structures can also be used as dissipative devices for earthquake-proof structures (Fraternali and Santos, 2019; Singh et al., 2020). In addition, tensegrity metamaterials can be used in impact protection and energy dissipation systems (Bauer et al., 2021; Ma et al., 2018).

A tensegrity should fulfill the following conditions (Zhang and Ohsaki, 2015): *i*) the tensegrity is free-standing without any support; *ii*) it is composed of only two types of members (cables in tension and struts in compression); *iii*) the struts are not in contact with each other at their ends, and *iv*) the self-weight of the tensegrity is negligibly small in comparison with the member forces. The tensegrity structures shown in this work fulfill all the conditions listed above. In practice, in addition to

the preceding conditions, tensegrity structures should satisfy some other requirements. Some examples of these requirements are: members should not intersect with each other, and both the buckling of the struts and the yielding of the cables must be prevented. There are some optimization methods that consider member intersection (Xu et al., 2016) and buckling constraints (Xu et al., 2018) in order to avoid these situations. The member intersection and the potential local buckling of compression members have not been considered in the present work.

The creation of these types of interesting structures is complex because tensegrities do not exhibit very intuitive principles (Gómez-Jáuregui, 2010). In addition, novel applications such as biomechanical structural models and mechanical metamaterials require large-scale tensegrity structures, which increase the complexity of the design procedure. One of the main sources of tensegrity structures are regular polyhedrons, including simple polyhedral tensegrities, prismatic tensegrities, and truncated polyhedral tensegrities (Yin et al., 2020; Zhang et al., 2019, 2021, 2013). However, truncated polyhedral tensegrities are limited by the five types of convex regular polyhedrons: tetrahedron, cube, octahedron, dodecahedron, and icosahedron.

Another way to construct a tensegrity structure is by assembling elementary modules together in a specific manner. In Murakami et al. (Murakami and Nishimura, 2001), the static and dynamic characterization of truncated regular polyhedral modules is studied. Rhode-

E-mail addresses: manuelalejandro.fernandez@uca.es (M.A. Fernández-Ruiz), emontes@ugr.es (E. Hernández-Montes), mlgil@ugr.es (L.M. Gil-Martín).

^{*} Corresponding author.

Barbarigos et al. (Rhode-Barbarigos et al., 2010) and Feron et al. (Feron et al., 2019) proposed the use of tensegrity modules as elementary building modules in the design of pedestrian bridges. In line with this design procedure, Li et al. (Li et al., 2010) show that tensegrity structures can be constructed by assembling one-bar elementary cells. Pugh (Pugh, 1976) defines two main classes of tensegrity structures, named "rhombic" (or "diamond") and "zig-zag" systems. Most rhombic and zig-zag tensegrities can be considered as assemblages of rhombic and Z-shaped cells, respectively (see Fig. 1).

Finally, tensegrity families are another great source of tensegrity structures. A tensegrity family is a group of tensegrity structures that share a common connectivity pattern (Fernández-Ruiz et al., 2022, 2021, 2020, 2019). The Octahedron (Fernández-Ruiz et al., 2022, 2019), the Z-Octahedron (Fernández-Ruiz et al., 2020), and the X-Octahedron (Fernández-Ruiz et al., 2021) families are examples of families of tensegrity structures found in the literature. The greatest advantage of the design of tensegrity structures based on tensegrity families is that they can be used to construct new tensegrity forms based on topology instead of using geometrical intuition. Each member of the family has all the previous members of the family as folded forms (Fernández-Ruiz et al., 2019). Folded forms are tensegrity structures where some nodes in the equilibrium configuration share the same position in the space (Hernández-Montes et al., 2018), while full forms are tensegrity structures where all the nodes have different positions in the equilibrium shape (Hernández-Montes et al., 2018). With this property in mind, a full form can be considered as the folded form of the subsequent member of the family, obtaining new tensegrities with a higher number of nodes, struts, and cables.

In this work, a new member of the Z-Octahedron family is presented: the Z-triple-expanded octahedron (which is composed of 48 nodes, 24 struts, and 72 cables). In addition, a new graphical representation of the members of the Z-Octahedron family based on octagonal cells is proposed. New tensegrity structures are constructed by changing the connectivity pattern of the members of the elementary octagonal cell of the Z-Octahedron family. Several element groupings have been considered in order to find different equilibrium configurations. An analytical formfinding method (Fernández-Ruiz et al., 2019; Hernández-Montes et al., 2018) based on the Force Density Method (FDM) (Linkwitz and Schek, 1971; Schek, 1974) is used to solve the self-equilibrated states of the tensegrities shown in this work. Finally, it has been proved that the introduction of additional cables in the octagonal cells can result in an improvement of the stability of a tensegrity.

The tensegrity structures presented in this work could have promising engineering applications. New research in different fields could be derived from the application of these new tensegrities. Among others examples, they could be considered as a unit of tensegrity mass-spring

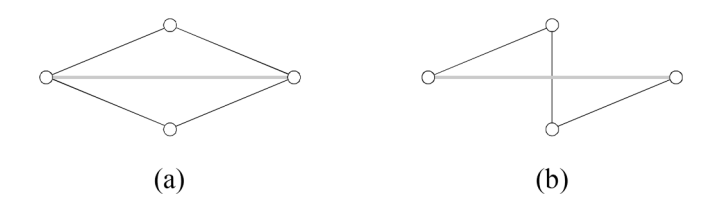


Fig. 1. Rhombic (a) and Z-shaped (b) elementary cells. Thick gray lines and thin black lines correspond to struts and cables, respectively. Adapted from (Fernández-Ruiz et al., 2020).

chains (Amendola et al., 2018; Fraternali et al., 2014).

2. A new graphical representation of the Z-Octahedron family

2.1. The Z-Octahedron family

The Z-Octahedron family has already been presented in Fernández-Ruiz et al. (Fernández-Ruiz et al., 2020). The first two members, the Z-expanded octahedron and the Z-double-expanded octahedron are defined by using Z-shaped elementary cells (see Fig. 2.a and b, respectively).

The analytical form-finding method based on FDM that is employed in this work for the design of tensegrity structures is summarized in Appendix A, as well as the stability and super-stability criterions.

In Fernández-Ruiz et al. (Fernández-Ruiz et al., 2020), two types of cables are identified (type 1 and type 2) in the two tensegrities of the Z-Octahedron family shown in Fig. 2. Consequently, two positive values of the force:length ratio are considered for cables (q_{c1} and q_{c2} for type 1 and type 2 cables, respectively). On the other hand, only one value of force: length ratio is considered for struts (q_b , negative). The force:length ratio, q, is defined as the ratio between the axial force and the length of each member of the tensegrity. Furthermore, two independent normalized force:length ratios taken as $Q_1 = -q_{c1}/q_b$ and $Q_2 = -q_{c2}/q_b$ are considered. Note that, by definition, Q_1 and Q_2 are positive.

The Z-expanded octahedron (see Fig. 2a) is composed of 6 Z-shaped cells (12 nodes, 6 struts, and 18 cables). The solutions given by the analytical form-finding method considering $q_{c1}=q_{c2}$ (and consequently, $Q_I=Q_2$) have already been presented in (Fernández-Ruiz et al., 2020): $Q_1=1/10\left(11-\sqrt{41}\right)$ and $Q_1=1/10\left(11+\sqrt{41}\right)$. Other solutions are obtained, but they are ruled out because Q_I has negative values or it is equal to zero. The solution $Q_1=1/10\left(11+\sqrt{41}\right)$ leads to a superstable equilibrium configuration (the Z-expanded octahedron, see Fig. 2a), while $Q_1=1/10\left(11-\sqrt{41}\right)$ leads to a tensegrity which cannot not be considered as being either super-stable (it does not fulfill condition (ii) of the super-stability criterion) or stable (taking into consideration the material properties shown in Appendix A).

The next member of the Z-Octahedron family, the Z-double-expanded octahedron (see Fig. 2b) composed of 12 Z-shaped cells (24 nodes, 12 struts, and 36 cables), has already been presented in (Fernández-Ruiz et al., 2020). The solutions of the form-finding problem considering $q_{c1}=q_{c2}$ are $Q_1=1/10\left(11-\sqrt{41}\right)$, $Q_1=1/10\left(11+\sqrt{41}\right)$ and $Q_1=7/3$. The solution corresponding to $Q_1=7/3$ leads to the superstable full form of the Z-double-expanded octahedron (see Fig. 2b), $Q_1=1/10\left(11+\sqrt{41}\right)$, which corresponds to the unstable folded form of the Z-double-expanded octahedron, while $Q_1=1/10\left(11-\sqrt{41}\right)$ leads to an unstable tensegrity structure.

In Fernández-Ruiz et al. (Fernández-Ruiz et al., 2020), a higher number of different values of force:length ratio is studied.

2.2. Octagonal connection graphs

A plane connection graph is a graphical representation of the connectivity between the nodes of a tensegrity (Fernández-Ruiz et al., 2019). The plane connection graph has a key role in the design of tensegrity structures because it is the basis for the construction of connectivity matrix C (defined in Appendix A) of the tensegrity. Fig. 2 shows the plane connection graphs based on Z-shaped elementary cells of both

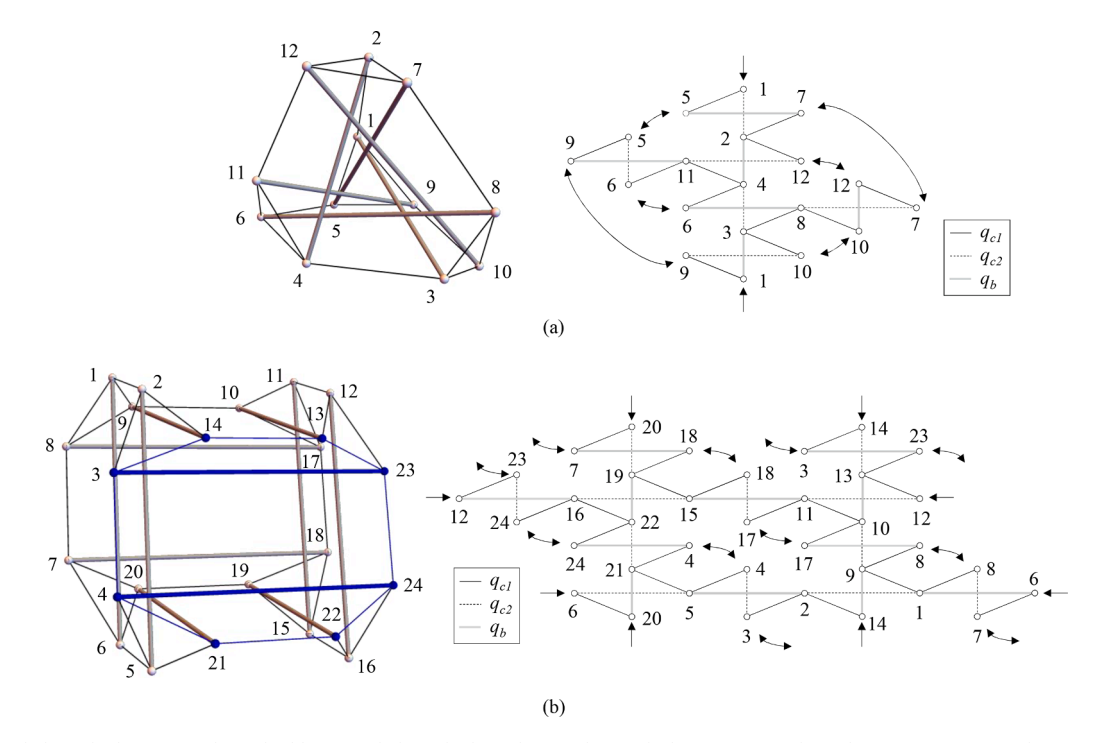


Fig. 2. A Z-expanded octahedron (a) and a Z-double-expanded-octahedron (b) together with their corresponding plane connection graphs. Gray lines, black lines, and dashed black lines correspond to struts, type 1 cables, and type-2 cables, respectively. The plane connection graphs have been adapted from (Fernández-Ruiz et al., 2020).

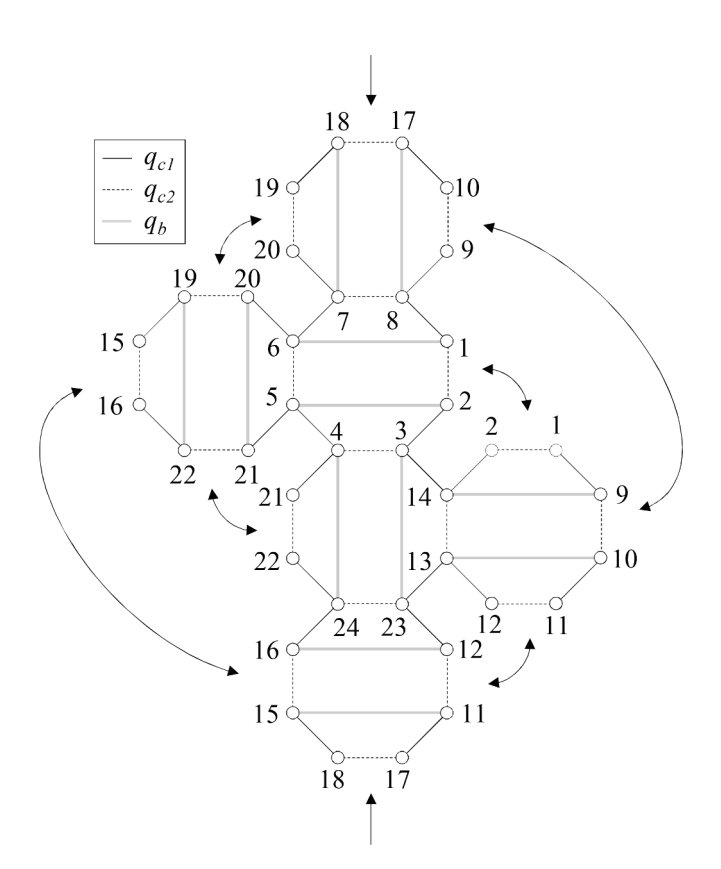


Fig. 3. New octagonal connection graph of the Z-double expanded octahedron. Gray lines, black lines, and dashed black lines correspond to struts, type 1 cables, and type-2 cables, respectively.

the Z-expanded octahedron and the Z-double expanded octahedron (Fernández-Ruiz et al., 2020). These plane connection graphs are obtained by replacing the rhombic cells of the tensegrities of the Octahedron family defined in (Fernández-Ruiz et al., 2019) by Z-shaped cells.

In this piece of work, an alternative plane connection graph is presented that is based on a new type of cell: the octagonal cell. In Fig. 2b, two struts and eight cables of the Z-double-expanded octahedron have been highlighted in blue (for the interpretation of the references to color, the reader is referred to the online version of this article). These struts and cables can be considered as making up an octagonal cell. Accordingly, the Z-double expanded octahedron can be constructed by assembling six octagonal cells (see Fig. 3). This new plane connection

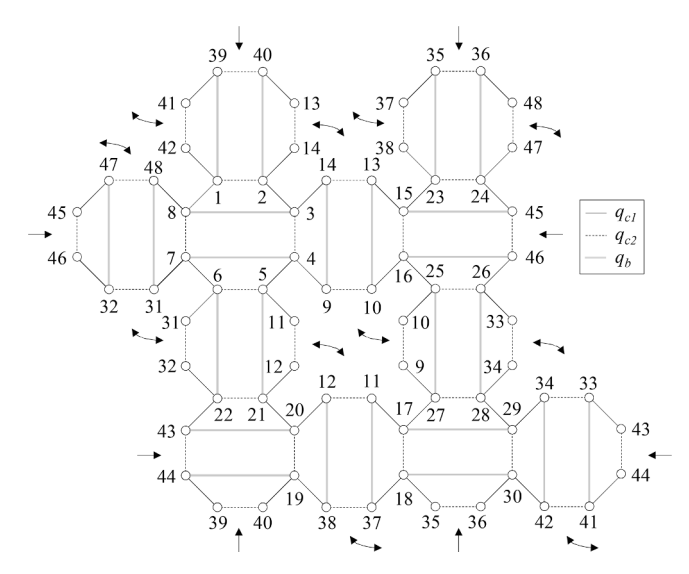


Fig. 4. Octagonal connection graph of the Z-triple-expanded octahedron. Gray lines, black lines, and dashed black lines correspond to struts, type 1 cables, and type-2 cables, respectively.

graph (called an octagonal connection graph) is equivalent to the one shown in Fig. 2b.

It should be highlighted that each of the elementary cells shown in Li et al. (Li et al., 2010) and those used in the Octahedron (Fernández-Ruiz et al., 2022; Fernández-Ruiz et al., 2019), the Z-Octahedron (Fernández-Ruiz et al., 2020), and the X-Octahedron (Fernández-Ruiz et al., 2021) tensegrity families only have one strut each. On the other hand, the new octagonal cell has two struts and eight cables. This new type of cell opens up a new range of possibilities for defining new tensegrity structures.

3. The Z-triple-expanded octahedron

It is interesting to note that the connectivity between the cells of the octagonal connection graph of the Z-double expanded octahedron (see Fig. 3) follows the same pattern as that of the Z-expanded octahedron that is based on Z-shaped elementary cells (see Fig. 2a). Therefore, the octagonal connection graph of the Z-triple expanded octahedron (see Fig. 4) has been constructed following the same connection pattern as that of the Z-double-expanded octahedron when Z-shaped cells are considered (see Fig. 2b).

Fig. 4 shows that the Z-triple-expanded octahedron is composed of 12 octagonal cells (48 nodes, 24 struts, and 72 cables). For this tensegrity, the solutions of the form-finding problem $areQ_1=1/10\left(11-\sqrt{41}\right), Q_1=1/10\left(11+\sqrt{41}\right), Q_1=7/3, Q_1=2/5, Q_1=1/7\left(10-\sqrt{30}\right)$ and $Q_1=1/7\left(10+\sqrt{30}\right)$. The solutions $Q_1=1/10\left(11+\sqrt{41}\right)$ and $Q_1=7/3$ correspond to the Z-expanded octahedron and the Z-double-expanded octahedron, whose members are duplicated and quadruplicated, (the first one is unstable and the second one is superstable), respectively. Therefore, it can be concluded that the Z-triple-expanded octahedron resulting from the octagonal connection graph shown in Fig. 4 belongs to the Z-Octahedron family. It has been verified that the solutions $Q_1=1/10\left(11-\sqrt{41}\right), Q_1=2/5$ and $Q_1=1/7\left(10-\sqrt{41}\right)$

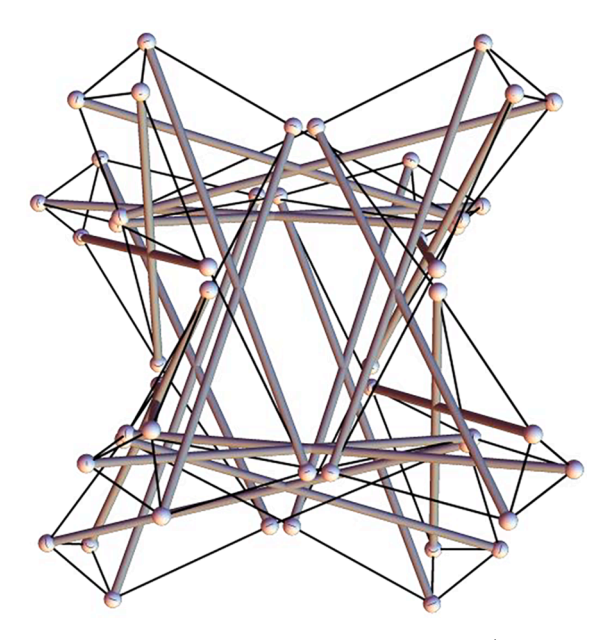


Fig. 5. Z-triple-expanded octahedron with $Q_1=1/7$ (10+ $\sqrt{30}$) and $q_b=-1$.

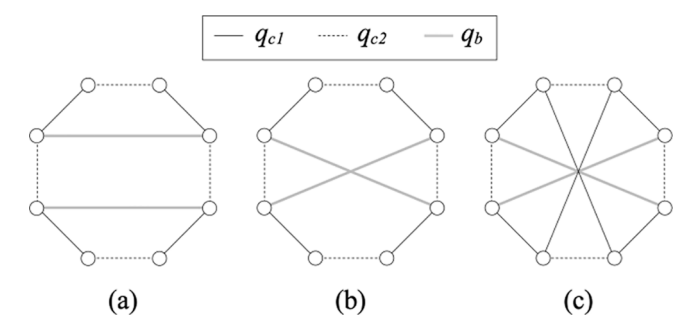


Fig. 6. Octagonal cell type 1 (a), type 2 (b), and type 3 (c). Gray lines, black lines, and dashed black lines correspond to struts, type 1 cables, and type-2 cables, respectively.

 $\sqrt{30}$) correspond to unstable tensegrity structures. The solution $Q_1=1/7(10+\sqrt{30})$ leads to the full-form of the Z-triple-expanded octahedron (see Fig. 5), which is not super-stable because its corresponding force density matrix, ${\bf D}$, is not positive semi-definite (in this case some eigenvalues are very close to 0, but they are negative). However, and according to the material properties shown in Appendix A, the Z-triple-expanded octahedron is a stable tensegrity.

4. New tensegrity structures based on the Z-Octahedron family

New tensegrity structures can be defined by replacing the connectivity pattern of the elementary octagonal cells of the plane connection graphs of the Z-Octahedron family. Let us consider, in addition to the previously considered octagonal cell (see Figs. 3 and 4 and the type 1 octagonal cell in Fig. 6.a), another two types of octagonal cells (see types 2 and 3 in Fig. 6). Fig. 6 shows that the struts are crossed in a type 2 octagonal cell, and two additional crossed cables connecting opposite nodes of the cell are included in a type 3 cell.

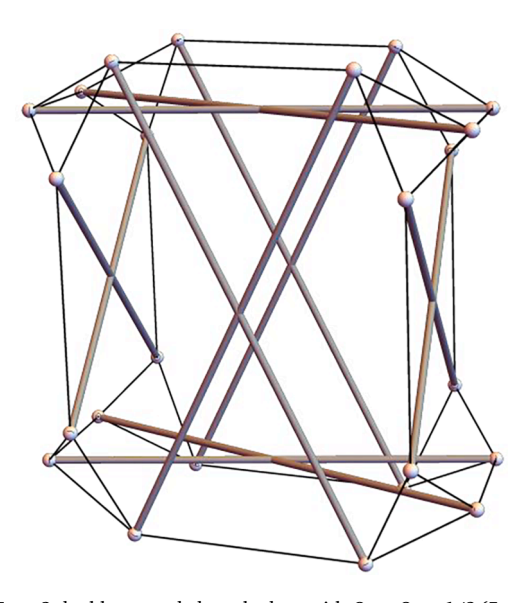


Fig. 7. Type-2-double-expanded octahedron with $Q_1=Q_2=1/3$ (5+ $\sqrt{13}$) and $q_b=$ -1.

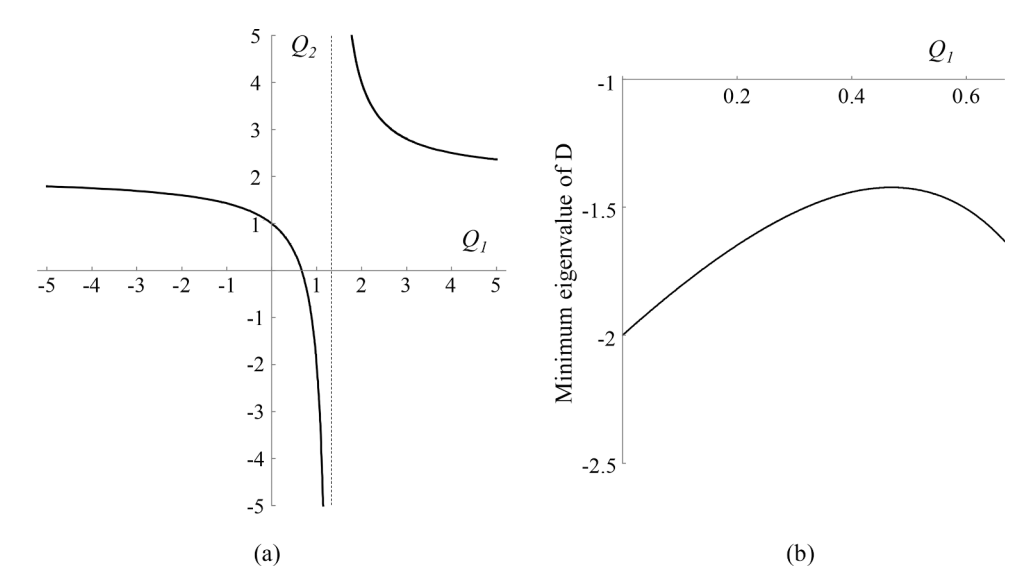


Fig. 8. $Q_1 - Q_2$ self-equilibrium curves of the type-2-double-expanded octahedron (Eq. (1)) (a) and minimum eigenvalue of D for the $Q_1 - Q_2$ graph of Eq. (1) in the region $0 < Q_1 < 2/3$, considering $q_b = -1$.

4.1. Type 2 octagonal cell

4.1.1. Type-2-double-expanded octahedron

The plane connection graph of the type-2-double-expanded octahedron is obtained by replacing the type 1 octagonal cells from Fig. 3 with type 2 octagonal cells (Fig. 6b).

If only two values of q are considered $(q_{c1}=q_{c2})$, and so $Q_1=Q_2$), the solutions of the form-finding problem that lead to a full form of the tensegrity are: $Q_1=1/3\big(5-\sqrt{13}\,\big)$ and $Q_1=1/3\big(5+\sqrt{13}\,\big)$. The solution $Q_1=1/3\big(5-\sqrt{13}\,\big)$ leads to an unstable tensegrity but, for $Q_1=1/3\big(5+\sqrt{13}\,\big)$, a super-stable tensegrity is obtained: the type-2-double-expanded octahedron (see Fig. 7).

If three values of q are considered instead of two, as indicated in Fig. 6b (q_{c1} , q_{c2} and q_b), then the solution of the form-finding problem is the one shown in Eq. (1). It should be highlighted that other solutions can also be obtained, but they have been ruled out because they lead to folded forms, or because Q_1 and/or Q_2 have negative values (and by definition, both must be positive).

$$Q_2 = \frac{2(-2+3Q_1)}{-4+3Q_1} \tag{1}$$

Fig. 8.a shows the curve, $Q_I - Q_2$, which corresponds to Eq. (1). It is important to note that not all the $Q_I - Q_2$ pairs resulting from Eq. (1) lead to super-stable or stable tensegrities. Hence, the next step is to study whether the super-stability conditions numbered in Appendix A are fulfilled or not. First of all, the conditions $Q_I > 0$ and $Q_2 > 0$ are checked.

Table 1 Super-stability analysis of the type-2-double-expanded octahedron considering three values of q. Condition (i): force density matrix D has exactly-four zero-eigenvalues. Condition (ii): matrix D is positive semi-definite. Condition (iii): geometry matrix G has a rank of 6.

Solution	Q_1 and $Q_2 > 0$	Condition (i)	Condition (ii)	Condition (iii)
Eq. (1)	$0 < Q_1 < 2/3$	1	×	_
	$Q_1 > 4/3$	✓	✓	✓

In the regions $0 < Q_1 < 2/3$ and $Q_1 > 4/3$, both Q_1 and Q_2 are positive. Secondly, condition (i) of the super-stability criterion is imposed on the structure, for which the rank deficiency of the resulting matrix D must be exactly d + 1 (d = 3 in three-dimensional tensegrities, see Appendix A). It has been verified that all the tensegrity structures in the regions 0 < $Q_1 < 2/3$ and $Q_1 > 4/3$ have exactly 4 zero eigenvalues. Condition (ii) of the super-stability criterion indicates that matrix \boldsymbol{D} must be positive semi-definite. This condition is fulfilled in region $Q_1 > 4/3$. Fig. 8.b shows the minimum eigenvalue of matrix **D** for all the $Q_1 - Q_2$ pairs obtained from Eq. (1) in region $0 < Q_1 < 2/3$, considering $q_b = -1$. It can be seen that there is always a negative eigenvalue and so tensegrity forms resulting from Eq. (1) in region $0 < Q_1 < 2/3$ do not fulfill condition (ii) of super-stability. Finally, and according to condition (iii) of the super-stability criterion, the rank of the geometry matrix, G, must be $(d^2+d)/2=6$. The tensegrity forms obtained from Eq. (1) in region Q_1 > 4/3 have a geometry matrix with a rank of six. Consequently, the tensegrities of region $Q_1 > 4/3$ can be considered as super-stable. On the contrary, tensegrity forms obtained from Eq. (1) in region $0 < Q_1 < 2/3$ are unstable. The study of the super-stability is summarized in Table 1.

Fig. 9 shows three super-stable equilibrium configurations of the type-2-double-expanded octahedron for different $Q_1 - Q_2$ pairs of Eq. (1) in region $Q_1 > 4/3$. As Q_1 increases in Eq. (1), the resultant tensegrity resembles more a truncated cube (see Fig. 9).

4.1.2. Type-2-triple-expanded octahedron

As previously mentioned, the plane connection graph of the type-2-triple-expanded octahedron is constructed by replacing the type 1 octagonal cells from Fig. 4 with type 2 octagonal cells. It should be highlighted that the connectivity pattern between the type 2 octagonal cells in the type-2-triple-expanded octahedron is the same as the one that corresponds to the Z-triple-expanded octahedron (see Fig. 4). If only two values of q are considered ($Q_1=Q_2$), the solutions of the form-finding problem that leads to a full-form are $Q_1=3/70\left(31-3\sqrt{29}\right)$ and $Q_1=3/70\left(31+3\sqrt{29}\right)$. Both solutions lead to unstable tensegrity forms. Other solutions are also obtained, including $Q_1=1/3\left(5+\sqrt{13}\right)$, which corresponds to the type-2-double-expanded octahedron, whose nodes and members are duplicated (folded form). Given the complexity

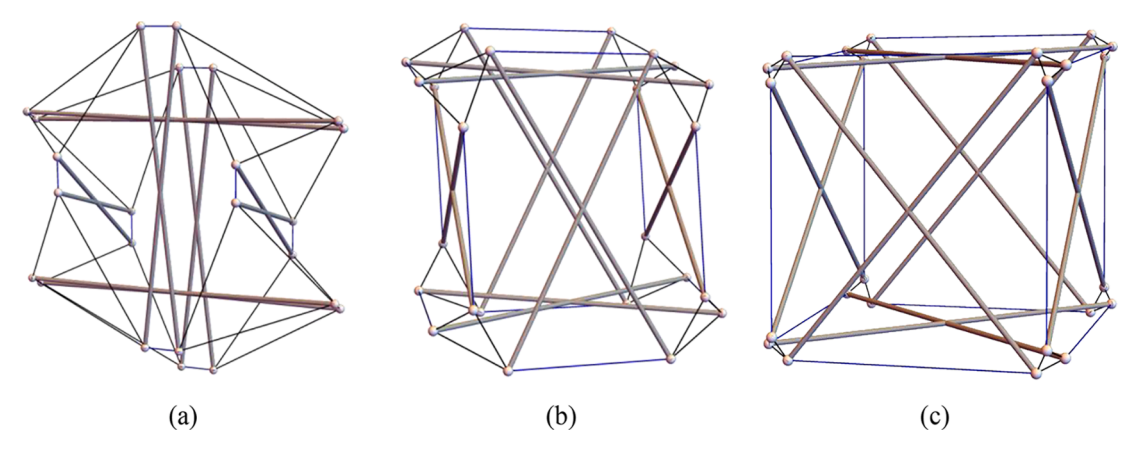


Fig. 9. Equilibrium shapes of the type-2-double-expanded octahedron considering different values of q. $Q_1 = 1.5 & Q_2 = 10$ (Eq. (1)) & $q_b = -1$ (a); $Q_1 = 3 & Q_2 = 2.8$ (Eq. (1)) & $q_b = -1$ (b); $Q_1 = 8 & Q_2 = 2.2$ (Eq. (1)) & $q_b = -1$ (c). Black and blue cables correspond to q_{c1} and q_{c2} , respectively and gray bars to q_b . (For interpretation of the references to color in this figure legend, the reader is referred to the web version of this article.)

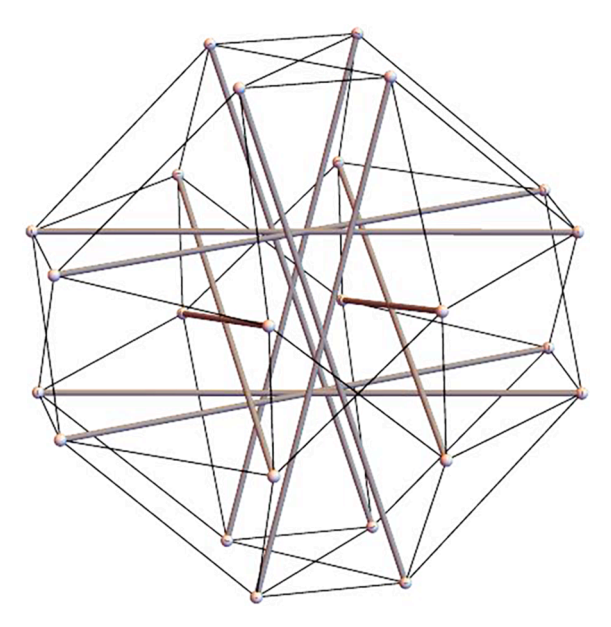


Fig. 10. Type-3-double-expanded octahedron with $Q_I=Q_2=1/17$ (15+ $\sqrt{89}$) and $q_b=$ -1.

of the system of equations obtained, a higher number of different values of q are not considered due to the high computational cost. limitations in the calculation capacity.

4.2. Octagonal cell type 3

4.2.1. Type-3-double-expanded octahedron

As in the previous case, the plane connection graph of the type-3-double-expanded octahedron is obtained by replacing the type 1 octagonal cells of Fig. 3 with type 3 octagonal cells (Fig. 6c). The type 3 double-expanded octahedron is composed of 6 type-3 octagonal cells (24

nodes, 12 struts, and 48 cables). The solutions of the form-finding problem that consider $q_{c1}=q_{c2}$ (and consequently $Q_1=Q_2$) that lead to a full form are $Q_1=1/17\big(15-\sqrt{89}\big)$ and $Q_1=1/17\big(15+\sqrt{89}\big)$. Solution $Q_1=1/17\big(15-\sqrt{89}\big)$ leads to an unstable tensegrity, but $Q_1=1/17\big(15+\sqrt{89}\big)$ corresponds to a super-stable tensegrity called type-3-double-expanded octahedron (see Fig. 10).

If three values of q are considered, as indicated in Fig. 6c (q_{c1} , q_{c2} and q_b), the only solution that leads to full forms is shown in Eq. (2).

$$Q_2 = \frac{2(4 - 11Q_1 + 5Q_1^2)}{8 - 7Q_1} \tag{2}$$

Fig. 11.a shows the Q_I-Q_2 representation that corresponds to Eq. (2). As in Section 4.1.1, a study of the super-stability is carried out depending on the value of the Q_I-Q_2 pairs (this study is summarized in Table 2). Tensegrity structures for which $8/7 < Q_I < 1/10 \left(11 + \sqrt{41}\right)$ can be considered as super-stable while if $0 < Q_I < 1/10 \left(11 + \sqrt{41}\right)$, then the tensegrities are unstable.

Fig. 12 shows three super-stable equilibrium configurations of the type-3-double-expanded octahedron considering several $Q_I - Q_2$ pairs of Eq. (2) in region $8/7 < Q_I < 1/10(11 + \sqrt{41})$.

4.2.2. Type-3-triple-expanded octahedron

The plane connection graph of the type-3-triple-expanded octahedron is constructed by replacing the type 1 octagonal cells from Fig. 4 with type 3 octagonal cells. The connectivity pattern between the type 3 octagonal cells in the type-3-triple-expanded octahedron is the same than the one corresponding to the Z-triple-expanded octahedron (see Fig. 4) and to the type-2-triple-expanded octahedron. The type-3-triple-expanded octahedron is composed of 12 type 3 octagonal cells (48 nodes, 24 struts, and 96 cables). As in Section 4.1.2, only two values of q are considered $(q_{c1}=q_{c2},$ and so $Q_1=Q_2)$ due to the high computational cost. The solutions of the form-finding problem that lead to a full-form are $Q_1=1/346\left(379+3\sqrt{3581}\right)$ and $Q_1=1/346\left(379-3\sqrt{3581}\right)$. The solution $Q_1=1/346\left(379-3\sqrt{3581}\right)$ leads to an unstable tensegrity, but the solution $Q_1=1/346\left(379+3\sqrt{3581}\right)$ corresponds to a

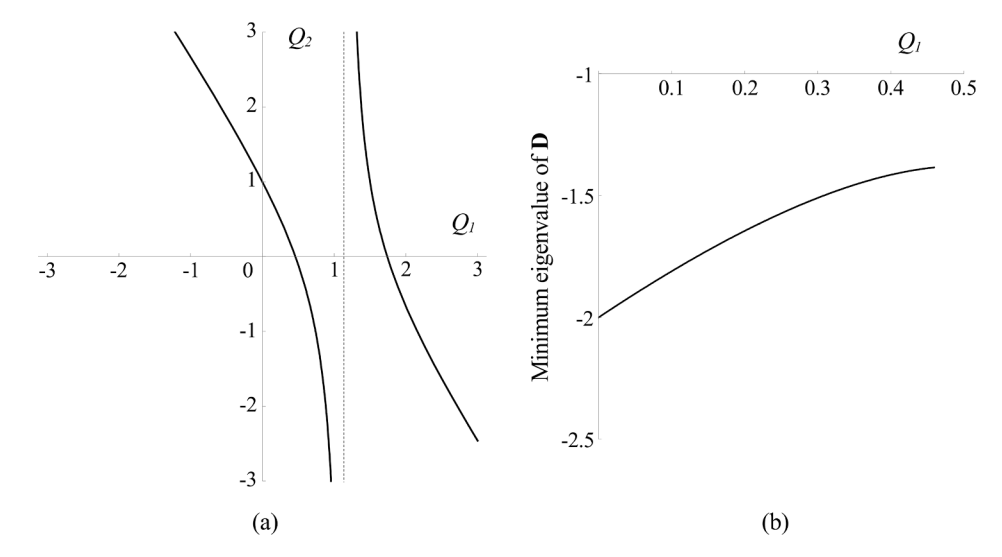


Fig. 11. $Q_I - Q_2$ self-equilibrium curves of the type-3-double-expanded octahedron (Eq. (2)) (a) and the minimum eigenvalue of D for the $Q_I - Q_2$ graph of Eq. (2) in region $0 < Q_I < 1/10$ (11- $\sqrt{41}$) considering $q_b = -1$.

Table 2 Super-stability analysis of the type-3-double-expanded octahedron considering three values of q. Condition (i): force density matrix D has exactly-four zero-eigenvalues. Condition (ii): matrix D is positive semi-definite. Condition (iii): geometry matrix G has a rank of 6.

Solution	Q_1 and $Q_2 > 0$	Condition (i)	Condition (ii)	Condition (iii)
Eq. (2)	$0 < Q_1 < 1/10 $ (11- $\sqrt{41}$)	1	×	-
	$8/7 < Q_1 < 1/10$ $(11+\sqrt{41})$	✓	1	1

super-stable tensegrity called type-3-triple-expanded octahedron (see Fig. 13). Other solutions are also obtained, including $Q_1 = 1/17(15 + \sqrt{89})$, which corresponds to the type-3-double-expanded octahedron, whose nodes and members are duplicated (folded form).

It is interesting to note that the introduction of additional cables means an improvement in the stability of the tensegrity because the type-2-triple-expanded octahedron is unstable, while the type-3-triple-expanded octahedron is a super-stable tensegrity. Hence, the type of octagonal elementary cell used to construct the connectivity pattern has a significant amount of influence on the tensegrity obtained, especially related to number of cables or tensioned members. The introduction of these two cables per octagonal cell is responsible for the difference in the stability of type 2 and type 3 triple-expanded octahedron tensegrity structures.

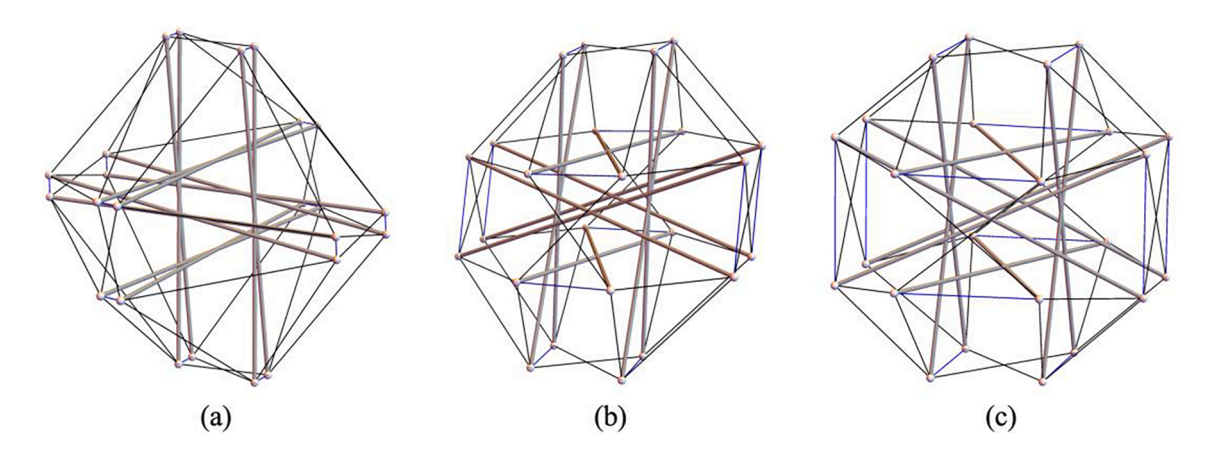


Fig. 12. Equilibrium shapes of the type-3-double-expanded octahedron considering different values of q. $Q_1=1.2$ & $Q_2=10$ (Eq. (2)) & $q_b=-1$ (a); $Q_1=1.5$ & $Q_2=1$ (Eq. (2)) & $q_b=-1$ (b); $Q_1=1.7$ & $Q_2=0.13$ (Eq. (2)) & $q_b=-1$ (c). Black and blue cables correspond to q_{c1} and q_{c2} , respectively and gray bars to q_b . (For interpretation of the references to color in this figure legend, the reader is referred to the web version of this article.)

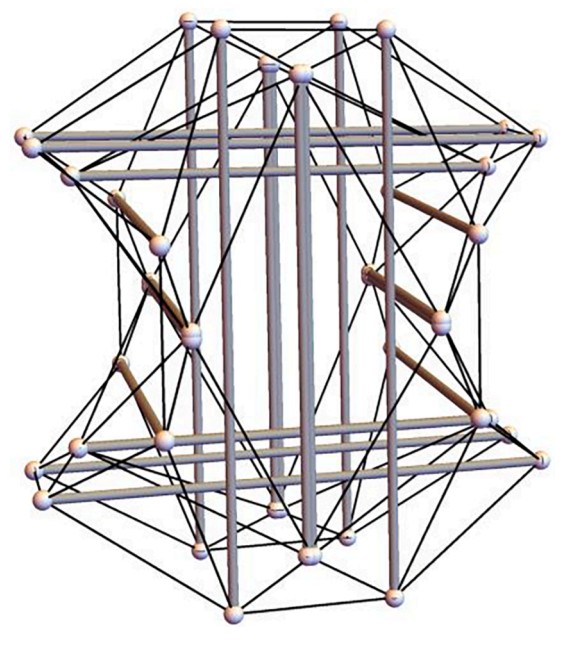


Fig. 13. Type-3-triple-expanded octahedron with $Q_1=Q_2=1/346$ (379 $+3\sqrt{3581}$) and $q_b=-1$.

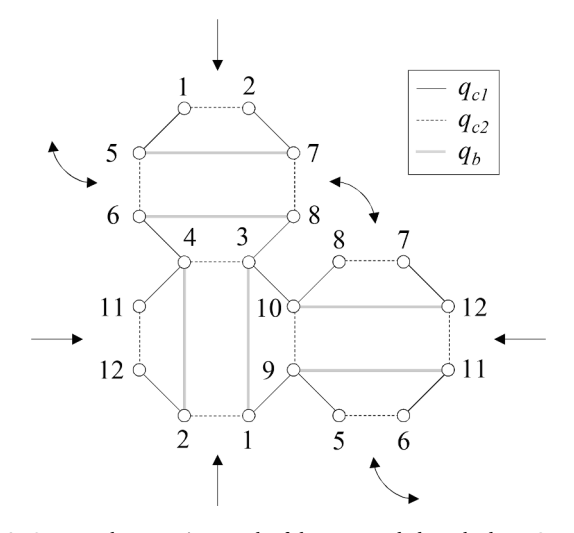


Fig. 14. Octagonal connection graph of the Z-expanded octahedron. Gray lines, black lines, and dashed black lines correspond to struts, type 1 cables, and type-2 cables, respectively.

4.3. Octagonal connection graphs for the expanded octahedron

Special attention is paid to the Z-expanded octahedron (Fig. 2a) when an octagonal elementary cell is used. Fig. 14 shows the octagonal connection graph of the Z-expanded octahedron (which is equivalent to the one shown in Fig. 2a). The comparison of this figure with Figs. 3 and 4 shows that, in Fig. 14, some of the external nodes are permuted, and so the connection pattern is slightly different.

As in the previous sections, the type-1 octagonal cells in Fig. 14 have been replaced by type 2 and type 3 octagonal cells (see Fig. 6), and just one or two values of the force:length ratios for cables have been considered. The results obtained that correspond to super-stable tensegrities are summarized in Table 3.

Table 3 shows that the solution of the form-finding problem of type 1 and type 2 expanded octahedrons is exactly the same. In addition, this solution has been studied in Fernández-Ruiz et al. (Fernández-Ruiz et al., 2020). On the other hand, Fig. 15 shows several equilibrium configurations of the type-3-expanded octahedron that consider different $Q_I - Q_2$ pairs.

4.4. Summary

All the values of the force:length ratios obtained in this work which lead to stable or super-stable full-forms of tensegrities are summarized in Fig. 16.

5. Conclusions

The Z-expanded octahedron and the Z-double-expanded octahedron are constructed by assembling Z-shaped cells. In this piece of work, a new graphical representation of the members of the Z-Octahedron family based on octagonal cells has been proposed. This new type of elementary cell has eight nodes and two struts, twice the number of nodes and struts than those found in rhombic and Z-shaped cells. The Z-triple-expanded octahedron has been obtained from the topology of the Z-Octahedron family considering the new octagonal connection graphs. This stable tensegrity structure is composed of 48 nodes, 24 struts, and 72 cables. The Z-triple-expanded octahedron contains both the Z-double-expanded octahedron and the Z-expanded octahedron as folded forms, which is a necessary condition for tensegrity families belonging to the same family. It has been proved that the new octagonal graphical representation of the Z-Octahedron family can be a good source of new tensegrity forms.

New tensegrity structures derived from the Z-Octahedron family have been defined. The connections between elements of the new octagonal cells have been modified leading to other types of octagonal cells (type 2 and type 3 octagonal cells). Super-stable tensegrity forms have been obtained analytically. In addition, several element groupings have been considered in order to obtain different equilibrium

Table 3 Z-expanded octahedron. Summary of super-stable configurations.

Octagonal cell	$Q_1 = Q_2 = -q_{c1}/q_b$	$Q_{I} = -q_{cI}/q_{b} \& Q_{2} = -q_{c2}/q_{b}$		
	Solution	Solution	Region	
Type 1 Type 2	$Q_1 = 1/10 ig(11 + \sqrt{41}ig)$	$Q_2 = \frac{-2 + 6Q_1 - 3Q_1^2 + \sqrt{4 - 8Q_1 + 8Q_1^2 - 12Q_1^3 + 9Q_1^4}}{4(-1 + Q_1)}$	$Q_1 > 1$	
Type 3	$Q_1 = 3/4$	$Q_2 = \frac{-2 + 10Q_1 - 11Q_1^2 + \sqrt{4 - 8Q_1 - 8Q_1^2 - 4Q_1^3 + 41Q_1^4}}{4(-1 + 2Q_1)}$	$1/2 < Q_1 < 1/10 \left(11 + \sqrt{41}\right)$	

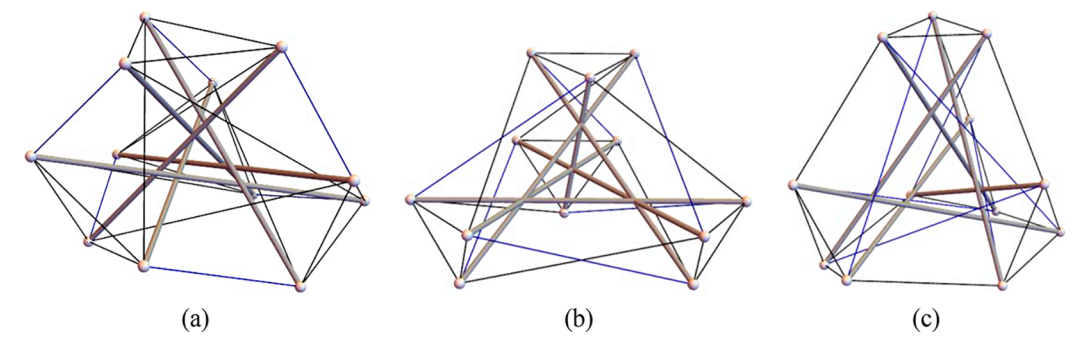


Fig. 15. Equilibrium shapes of the type-3- expanded octahedron considering different values of q according to Table 3. $Q_1 = 0.60 \& Q_2 = 1.15 \& q_b = -1$ (a); $Q_1 = 2.000 \& q_b = -1$ (b); $Q_1 = 1.60 \& Q_2 = 0.09 \& q_b = -1$ (c). Black and blue cables correspond to q_{c1} and q_{c2} , respectively and gray bars to q_b . (For interpretation of the references to color in this figure legend, the reader is referred to the web version of this article.)

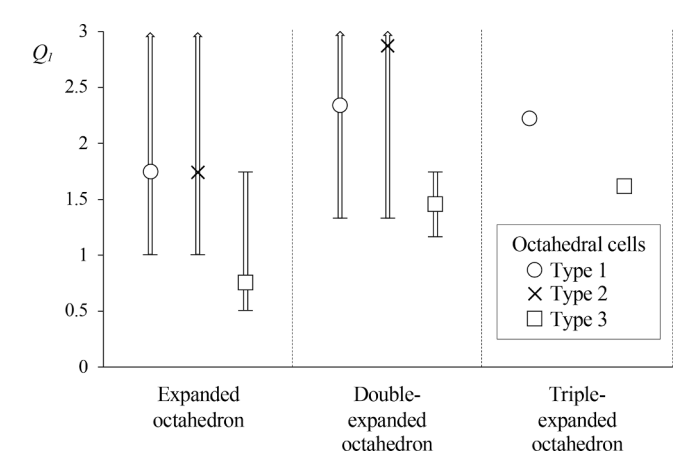


Fig. 16. Range of values of Q_I for which stable and super-stable tensegrities are obtained for all the types of octagonal cells studied in the work (see Fig. 6). Circles, crosses, and squares indicate the $Q_I - Q_2$ pair for which $Q_I = Q_2$ in the case of type 1, type 2, and type 3 octagonal cells respectively.

configurations of these new tensegrity structures. The introduction of additional cables in the elementary octagonal cell clearly results in an improvement of the stability of the resultant tensegrity and in a reduction of the force:length ratio in the cables in the equilibrium configuration.

Declaration of Competing Interest

The authors declare that they have no known competing financial interests or personal relationships that could have appeared to influence the work reported in this paper.

Appendix A

Analytical form-finding of tensegrity structures (Fernández-Ruiz et al., 2019; Hernández-Montes et al., 2018)

An in-depth explanation of the analytical form-finding method of tensegrity structures employed in this work can be seen in (Fernández-Ruiz et al., 2019; Hernández-Montes et al., 2018). In this appendix, a summary of this method is presented.

The FDM (Linkwitz and Schek, 1971; Schek, 1974) is one of the most commonly used form-finding methods for general pin-jointed networks. The highly non-linear equilibrium equations are linearized by introducing the concept of force density or force:length ratio. The force:length ratio, q, is defined as the ratio between the axial force and the length of each member of the tensegrity. The equilibrium equations of a general tensegrity composed of n nodes and m members (cables and struts) can be formulated as (Tran and Lee, 2010; Zhang and Ohsaki, 2015):

$$\mathbf{D}\mathbf{x} = 0 \\
\mathbf{D}\mathbf{y} = 0 \\
\mathbf{D}\mathbf{z} = 0$$
(A.1)

In Eq. (A.1) $\mathbf{D} = \mathbf{C}^T \mathbf{Q} \mathbf{C}$ ($\in \mathbb{R}^{n \times n}$) is the force density matrix, and \mathbf{x} , \mathbf{y} , \mathbf{z} ($\in \mathbb{R}^n$) are the nodal coordinate vectors. The symbol []^T represents the transpose operation of a matrix or vector. The inputs of the form-finding problem are connectivity matrix \mathbf{C} and the force:length ratio, q, of each member of the tensegrity. Connectivity matrix \mathbf{C} ($\in \mathbb{R}^{m \times n}$) defines the connectivity between the nodes of the tensegrity. This matrix is constructed as follows: if a general member of j connects nodes i and k (with i < k), the ith and kth elements of the jth row of \mathbf{C} are set to 1 and -1, respectively. Plane connection graphs are used to define matrix \mathbf{C} . On the other hand, vector $\mathbf{q} = (q_1, q_2, ..., q_m)$ ($\in \mathbb{R}^m$) contains the force:length ratio of each member of the tensegrity (\mathbf{Q} is the diagonal square matrix of vector \mathbf{q}).

In order to guarantee that a tensegrity does not lie in a space which has lower dimensions than the specific dimension d, matrix \mathbf{D} should have rank deficiency of at least d+1 (non-degeneracy condition (Hernández-Montes et al., 2018; Zhang and Ohsaki, 2006)). This non-degeneracy condition is achieved by making sure that the characteristic polynomial of \mathbf{D} (see Eq. (A.2)) has at least d+1 zero roots. Consequently, and in order to obtain a three-dimensional tensegrity (d=3), coefficients a_3 , a_2 , a_1 and a_0 of the characteristic polynomial must be zero. Coefficient a_0 is always zero because matrix \mathbf{D} is singular. Coefficients a_3 , a_2 and a_1 are expressed in terms of the force:length ratios of the members of the tensegrity (a_1 , a_2 , a_1 , a_2 , a_2 , a_3 , a_4 , a_4 , a_5 ,

$$p(\lambda) = \lambda^n + a_{n-1}\lambda^{n-1} + \dots + a_1\lambda + a_0$$
 (A.2)

$$a_3(q_1, ..., q_m) = 0$$

 $a_2(q_1, ..., q_m) = 0$
 $a_1(q_1, ..., q_m) = 0$
(A.3)

Stability, prestress-stability and super-stability of tensegrity structures

A tensegrity is stable if its corresponding tangent stiffness matrix $K = K_{GEOM} + K_{ELAST}$ is a positive semi-definite matrix (Fernández-Ruiz et al., 2019; Zhang and Ohsaki, 2015, 2007). Matrix K_{ELAST} is the elastic stiffness matrix and K_{GEOM} is the geometric stiffness matrix. The stability of tensegrity structures, together with the definition of matrices K_{GEOM} and K_{ELAST} , has been discussed in detail in (Fernández-Ruiz et al., 2019; Zhang and Ohsaki, 2015, 2007). In order to study the stability of a tensegrity, the material properties, A, (cross-sectional area) and, E, (Young's modulus) of its members must be known. In all the stability studies in this work, it is assumed that the maximum prestress is 1 % of EA (Zhang and Ohsaki, 2015).

In preliminary studies, it could be useful to know whether a tensegrity with a specific pre-stressed state is stable or not, without considering any specific materials. A tensegrity is said to be prestress-stable if it is stable in the state of self-equilibrium in the directions of infinitesimal mechanisms (Zhang and Ohsaki, 2015). In this prestress-stability criterion, it is assumed that the member stiffness of the tensegrity is high enough.

Super-stability is a much higher stability criterion than previous ones. It has been stated that a tensegrity is super-stable if it is always stable, regardless of material properties and prestress levels (Connelly, 1998; Zhang and Ohsaki, 2015, 2007). The super-stability conditions of tensegrity structures are as follows (Connelly, 1998; Zhang and Ohsaki, 2015, 2007):

- 1. The rank deficiency of the force density matrix **D** is exactly d + 1.
- 2. The force density matrix **D** is positive semi-definite.
- 3. The rank of the matrix **G** is $(d^2 + d)/2$.

An in-depth explanation on the geometry matrix G can be seen in (Zhang and Ohsaki, 2015).

References

- Bel Hadj Ali, N., Rhode-Barbarigos, L., Pascual Albi, A.A., Smith, I.F.C., 2010. Design optimization and dynamic analysis of a tensegrity-based footbridge. Eng. Struct. 32, 3650–3659. https://doi.org/10.1016/j.engstruct.2010.08.009.
- Amendola, A., Krushynska, A., Daraio, C., Pugno, N.M., Fraternali, F., 2018. Tuning frequency band gaps of tensegrity mass-spring chains with local and global prestress. Int. J. Solids Struct. 155, 47–56. https://doi.org/10.1016/j.ijsolstr.2018.07.002.
- Bauer, J., Kraus, J.A., Crook, C., Rimoli, J.J., Valdevit, L., 2021. Tensegrity metamaterials: toward failure-resistant engineering systems through delocalized deformation. Adv. Mater. 33, 1–9. https://doi.org/10.1002/adma.202005647.
- Boni, C., Royer-Carfagni, G., 2021. A new flexural-tensegrity bow. Mech. Mach. Theory 164, 104398. https://doi.org/10.1016/j.mechmachtheory.2021.104398.
- Chen, M., Goyal, R., Majji, M., Skelton, R.E., 2020. Design and analysis of a growable artificial gravity space habitat. Aerosp. Sci. Technol. 106, 106147 https://doi.org/ 10.1016/j.ast.2020.106147.
- Connelly, R., 1998. Tensegrity structures. Why are they stable? In: Thorpe, M.F.,
 Duxbury, P.M. (Eds.), Rigidity Theory and Applications. Kluwer Academic / Plenum
 Publishers, pp. 47–54.
- Fernández-Ruiz, M.A., Hernández-Montes, E., Carbonell-Márquez, J.F., Gil-Martín, L.M., 2019. Octahedron family: the double-expanded octahedron tensegrity. Int. J. Solids Struct. 165, 1–13. https://doi.org/10.1016/j.ijsolstr.2019.01.017.
- Fernández-Ruiz, M.A., Hernández-Montes, E., Gil-Martín, L.M., 2020. The Z-octahedron family: A new tensegrity family. Eng. Struct. 222, 111151 https://doi.org/10.1016/ j.engstruct.2020.111151.
- Fernández-Ruiz, M.A., Hernández-Montes, E., Gil-Martín, L.M., 2021. The Octahedron family as a source of tensegrity families: the X-octahedron family. Int. J. Solids Struct. 208–209, 1–12. https://doi.org/10.1016/j.ijsolstr.2020.10.019.
- Fernández-Ruiz, M.A., Hernández-Montes, E., Gil-Martín, L.M., 2022. Topological design of the octahedron tensegrity family. Eng. Struct. 259, 114211 https://doi.org/ 10.1016/j.engstruct.2022.114211.
- Feron, J., Boucher, L., Denoël, V., Latteur, P., 2019. Optimization of footbridges composed of prismatic tensegrity modules. J. Bridg. Eng. 24 https://doi.org/ 10.1061/(ASCE)BE.1943-5592.0001438.
- Fraldi, M., Cutolo, A., Carotenuto, A.R., Palumbo, S., Pugno, N., 2021. A lesson from earthquake engineering for selectively damaging cancer cell structures. J. Mech. Behav. Biomed. Mater. 119, 104533 https://doi.org/10.1016/j. imbbm.2021.104533.

- Fraternali, F., Carpentieri, G., Amendola, A., Skelton, R.E., Nesterenko, V.F., 2014. Multiscale tunability of solitary wave dynamics in tensegrity metamaterials. Appl. Phys. Lett. 105 https://doi.org/10.1063/1.4902071.
- Fraternali, F., Santos, F., 2019. Mechanical modeling of superelastic tensegrity braces for earthquake-proof structures. Extrem. Mech. Lett. 33, 100578 https://doi.org/ 10.1016/j.eml.2019.100578.
- Gómez-Jáuregui, V., 2010. Tensegrity structures and their application to architecture. PubliCan, Ediciones de la Universidad de Cantabria.
- Graells Rovira, A., Mirats Tur, J.M., 2009. Control and simulation of a tensegrity-based mobile robot. Rob. Auton. Syst. 57, 526–535. https://doi.org/10.1016/j. robot.2008.10.010.
- Hernández-Montes, E., Fernández-Ruiz, M.A., Gil-Martín, L.M., Merino, L., Jara, P., 2018. Full and folded forms: a compact review of the formulation of tensegrity structures. Math. Mech. Solids 23, 944–949. https://doi.org/10.1177/ 1081286517697372.
- Kan, Z., Peng, H., Chen, B., Xie, X., Sun, L., 2019. Investigation of strut collision in tensegrity statics and dynamics. Int. J. Solids Struct. 167, 202–219. https://doi.org/ 10.1016/j.ijsolstr.2019.03.012.
- Lee, H., Jang, Y., Choe, J.K., Lee, S., Song, H., Lee, J.P., Lone, N., Kim, J., 2020. 3D-printed programmable tensegrity for soft robotics. Sci. Robot. 5, 1–12. https://doi.org/10.1126/SCIROBOTICS.AAY9024.
- Li, Y., Feng, X.Q., Cao, Y.P., Gao, H., 2010. Constructing tensegrity structures from one-bar elementary cells. Proc. R. Soc. A Math. Phys. Eng. Sci. 466, 45–61. https://doi.org/10.1098/rspa.2009.0260.
- Linkwitz, K., Schek, H.J., 1971. Einige Bemerkungen zur Berechnung von vorgespannten Seilnetzkonstruktionen. Ingenieur-Archiv. 40, 145–158. https://doi.org/10.1007/ BF00532146.
- Liu, Y., Bi, Q., Yue, X., Wu, J., Yang, B., Li, Y., 2022. A review on tensegrity structures-based robots. Mech. Mach. Theory 168, 104571. https://doi.org/10.1016/j.mechmachtheory.2021.104571.
- Ma, Y., Zhang, Q., Dobah, Y., Scarpa, F., Fraternali, F., Skelton, R.E., Zhang, D., Hong, J., 2018. Meta-tensegrity: design of a tensegrity prism with metal rubber. Compos. Struct. 206, 644–657. https://doi.org/10.1016/j.compstruct.2018.08.067.
- Murakami, H., Nishimura, Y., 2001. Static and dynamic characterization of regular truncated icosahedral and dodecahedral tensegrity modules. Int. J. Solids Struct. 38, 9359–9381. https://doi.org/10.1016/S0020-7683(01)00030-0.
- Pugh, A., 1976. An introduction to tensegrity. University of California Press.

- Rhode-Barbarigos, L., Hadj Ali, N.B., Motro, R., Smith, I.F.C., 2010. Designing tensegrity modules for pedestrian bridges. Eng. Struct. 32, 1158–1167. https://doi.org/ 10.1016/j.engstruct.2009.12.042.
- Schek, H.J., 1974. The force density method for form-finding and computation of general networks. Comput. Methods Appl. Mech. Eng. 3, 115–134. https://doi.org/10.1016/0045-7825(74)90045-0.
- Singh, N., Amendola, A., Santos, F., Benzoni, G., Fraternali, F., 2020. Mechanical response of tensegrity dissipative devices incorporating shape memory alloys. IOP Conf. Ser. Mater. Sci. Eng. 999 https://doi.org/10.1088/1757-899X/999/1/012001.
- Suma, A., Coronel, L., Bussi, G., Micheletti, C., 2020. Directional translocation resistance of Zika xrRNA. Nat. Commun. 11, 1–9. https://doi.org/10.1038/s41467-020-17508-7
- Tibert, A.G., Pellegrino, S., 2002. Deployable tensegrity reflectors for small satellites. J. Spacecr. Rockets 39, 701–709. https://doi.org/10.2514/2.3867.
- Tran, H.C., Lee, J., 2010. Advanced form-finding of tensegrity structures. Comput. Struct. 88, 237–246. https://doi.org/10.1016/j.compstruc.2009.10.006.
- Veuve, N., Dalil Safaei, S., Smith, I.F.C., 2016. Active control for mid-span connection of a deployable tensegrity footbridge. Eng. Struct. 112, 245–255. https://doi.org/ 10.1016/j.engstruct.2016.01.011.
- Xu, X., Wang, Y., Luo, Y., 2016. General approach for topology-finding of tensegrity structures. J. Struct. Eng. 142, 04016061. https://doi.org/10.1061/(asce)st.1943-541x.0001532.

- Xu, X., Wang, Y., Luo, Y., Hu, D., 2018. Topology optimization of tensegrity structures considering buckling constraints. J. Struct. Eng. 144, 04018173. https://doi.org/ 10.1061/(asce)st.1943-541x.0002156.
- Yin, X., Gao, Z.Y., Zhang, S., Zhang, L.Y., Xu, G.K., 2020. Truncated regular octahedral tensegrity-based mechanical metamaterial with tunable and programmable Poisson's ratio. Int. J. Mech. Sci. 167, 105285 https://doi.org/10.1016/j. iimaccci. 2010.105285
- Zhang, L.Y., Li, Y., Cao, Y.P., Feng, X.Q., 2013. A unified solution for self-equilibrium and super-stability of rhombic truncated regular polyhedral tensegrities. Int. J. Solids Struct. 50, 234–245. https://doi.org/10.1016/j.ijsolstr.2012.09.024.
- Zhang, L.Y., Jiang, J.H., Wei, K., Yin, X., Xu, G.K., Zhang, J., 2021. Self-equilibrium and super-stability of rhombic truncated regular tetrahedral and cubic tensegrities using symmetry-adapted force-density matrix method. Int. J. Solids Struct. 233, 111215 https://doi.org/10.1016/j.ijsolstr.2021.111215.
- Zhang, J.Y., Ohsaki, M., 2006. Adaptive force density method for form-finding problem of tensegrity structures. Int. J. Solids Struct. 43, 5658–5673. https://doi.org/ 10.1016/j.ijsolstr.2005.10.011.
- Zhang, J.Y., Ohsaki, M., 2007. Stability conditions for tensegrity structures. Int. J. Solids Struct. 44, 3875–3886. https://doi.org/10.1016/j.ijsolstr.2006.10.027.
- Zhang, J.Y., Ohsaki, M., 2015. Tensegrity Structures. Form, Stability. and Symmetry. Springer.
- Zhang, J.Y., Ohsaki, M., Tsuura, F., 2019. Self-equilibrium and super-stability of truncated regular hexahedral and octahedral tensegrity structures. Int. J. Solids Struct. 161, 182–192. https://doi.org/10.1016/j.ijsolstr.2018.11.017.